β decay of neutron-rich ^{76}Cu and the structure of ^{76}Zn

U. Silwal,[1,2,*] J. A. Winger,[1] S. V. Ilyushkin,[1] K. P. Rykaczewski,[3] C. J. Gross,[3] J. C. Batchelder,[4] L. Cartegni,[5] I. G. Darby,[5] R. Grzywacz,[3,5] A. Korgul,[5,6,7] W. Królas,[8,7] S. N. Liddick,[5,9] C. Mazzocchi,[5,6,7] A. J. Mendez, II,[10] S. Padgett,[5] M. M. Rajabali,[5,11] D. P. Siwakoti,[1] D. Shapira,[3] D. W. Stracener,[3] and E. F. Zganjar[12]

[1]*Department of Physics and Astronomy, Mississippi State University, Mississippi State, Mississippi 39762, USA*
[2]*Department of Physics and Astronomy, University of Wyoming, Laramie, Wyoming 82701, USA*
[3]*Physics Division, Oak Ridge National Laboratory, Oak Ridge, Tennessee 37831, USA*
[4]*Department of Nuclear Engineering, University of California, Berkeley, Berkeley, California 94702, USA*
[5]*Department of Physics and Astronomy, University of Tennessee, Knoxville, Tennessee 37996, USA*
[6]*Faculty of Physics, University of Warsaw, Warsaw PL 02-093, Poland*
[7]*Joint Institute for Nuclear Physics and Applications, Oak Ridge, Tennessee 37831, USA*
[8]*Institute of Nuclear Physics, Polish Academy of Sciences, Kraków PL 31-342, Poland*
[9]*National Superconduction Cyclotron Laboratory, Michigan State University, East Lansing, Michigan 48824, USA*
[10]*Department of Chemistry and Physics, Campbell University, Buies Creek, North Carolina 27506, USA*
[11]*Physics Department, Tennessee Technological University, Cookeville, Tennessee 38505, USA*
[12]*Department of Physics and Astronomy, Louisiana State University, Baton Rouge, Louisiana 70803, USA*

(Received 2 March 2020; revised 7 July 2022; accepted 2 September 2022; published 13 October 2022)

The β decay of ^{76}Cu to the levels of ^{76}Zn was studied at the Holifield Radioactive Ion Beam Facility (HRIBF) at Oak Ridge National Lab (ORNL). A purified ^{76}Cu beam was developed and data were recorded for the decay of the $A = 76$ decay chain using four high-purity germanium (HPGe) clover detectors at the Low-energy Radioactive Ion Beam Spectroscopy Station (LeRIBSS). In this measurement, data on γ-ray emission following β decay, including $\beta\gamma$ and $\gamma\gamma$ coincidences, were collected and $\gamma\gamma$ spectra were analyzed to identify the statistically significant coincidences. From this analysis, we propose a level scheme for ^{76}Zn which contains a total of 59 energy levels up to 6.0 MeV containing 105 γ rays. We have identified an additional 53 γ rays associated with this decay which could not be place in the decay scheme due to insufficient coincidence information or no energy match to identified levels. No γ rays from states in ^{75}Zn fed in the delayed-neutron branch were observed even though other γ rays in the $A = 75$ decay chain were observed. Spin and parity assignments are proposed for some levels based on comparison to systematics and shell model calculations.

DOI: 10.1103/PhysRevC.106.044311

I. INTRODUCTION

There are substantial gaps in our knowledge of decay properties of neutron-rich nuclei despite previous spectroscopic efforts. Many of the neutron-rich nuclides above $Z = 20$ still remain beyond the reach of current facilities, hence there is a need to rely on theoretical models to predict their properties. It has been experimentally observed that the properties of nuclei near stability cannot always be extrapolated to get the properties of nuclides around the particle drip lines, but require some new aspect of the nuclear force to be considered [1–6]. The nuclides near the proton shell closure at $Z = 28$ with neutron number $N = 28$–50 approaching the doubly magic nuclide ^{78}Ni are interesting cases to study as they exhibit anomalous behavior such as shape deformation, coexistence, and triaxiallity [7–9]. A detailed study of nuclei in this region provides a test on the extent to which the predicted magic numbers remain valid for neutron-rich nuclides far from stability.

Beyond nuclear structure, understanding the β decays of neutron-rich fission products has a practical application in the nuclear energy industry where the energy released (*decay heat*) contributes to the total energy generated by the fission process. Although decay heat can be directly measured for any given reactor fuel composition, a better method would be to estimate the decay heat for any reactor fuel composition based on available nuclear data. Most of the β-decay data currently available come from high-resolution studies. With a large Q_β window, the decay fragments can feed a nearly continuous distribution of levels by allowed β decay. These levels emit a large number of very weak γ rays as they de-excite to the ground state, leading to what has been termed the *pandemonium effect* [10]. Due to efficiency limitations in the detector systems used, many weak and/or high-energy γ rays have not been identified. Hence, the detector system used has a significant influence on the completeness of the decay schemes developed. The β decay of ^{76}Cu is nearly ideal for the high-resolution measurement performed here to obtain a complete decay scheme. It has a large Q_β value, a high neutron separation energy, and a known β-delayed neutron branch indicating feeding to states up to the neutron separation energy. Although the experiment presented here cannot hope to measure the complete β-decay profile, the objective

*usilwal@uncc.edu

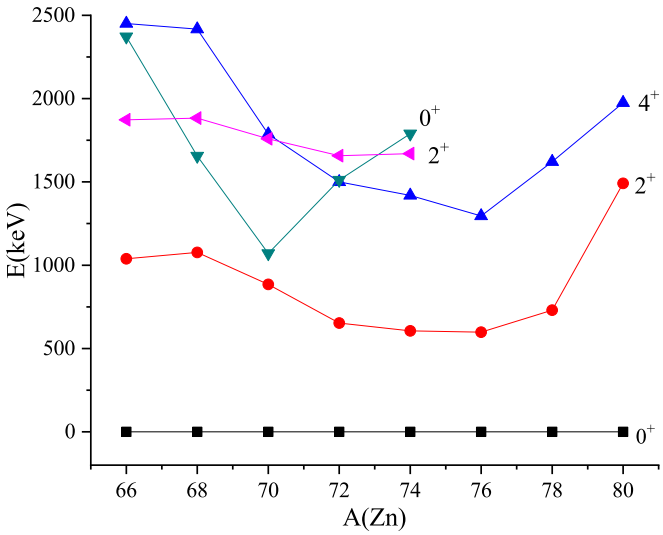

FIG. 1. Low-energy level systematics of zinc isotopes for mass (A) in the range from 66 to 80 [17–26].

is to better understand the limitations of high-resolution γ-ray spectroscopy to provide a complete decay scheme.

In the traditional shell model view of ^{76}Cu, the 29th proton should be in a $\pi 2p_{3/2}$ orbital while the 47th neutron is in the $\nu 1g_{9/2}$ orbital [11], suggesting a ground state spin-parity of $J^\pi = 3^-$ to 6^-. However, it is known in this region from theoretical arguments that the monopole interaction between $\nu 1g_{9/2}$ and $\pi 2p_{3/2}$ orbitals along with coupling to unbound states can result in the $\pi 1f_{5/2}$ orbital migrating to below the $\pi 2p_{3/2}$ orbital [12,13], suggesting a ground state spin-parity of 2^- is possible. A recent measurement by Groote *et al.* [14] indicates the ground state is in fact 3^-, suggesting the $\pi 2p_{3/2}$ orbital remains lower or at least the two orbitals combine to produce this state. This is in contrast to the result from Flanagan *et al.* [4] who measured a $\pi 1f_{5/2}$ ground state in ^{75}Cu. As shown in Fig. 1, the 2_1^+ states in the Zn isotopes remain almost constant above 1 MeV while neutrons fill the $\nu 1f_{5/2}$ and $\nu 2p_{3/2}$ orbitals but rapidly decrease in the energy as the $\nu 1g_{9/2}$ and $\nu 2p_{1/2}$ orbitals fill, reaching a minimum at 599 keV for ^{76}Zn [15,16] before rising rapidly to the shell closure at $N = 50$. The situation for the 4_1^+ state is similar, with a minimum at 1296 keV for $N = 46$. The 2_2^+ state shows only a slight drop in energy, reaching a minimum at $N = 42$ while hinting at a an increase in energy as the shell continues to fill. In contrast, the 0_2^+ state shows a sharp minimum at the $N = 40$ shell closure. It can be expected that the increased collectivity near mid-filling of the $\nu 1g_{9/2}$ orbital will result in coexistence of spherical and deformed structures. With this in mind, it is expected that the β decay of ^{76}Cu will feed negative parity states which will not directly deexcite to the ground state, but must instead connect through other states. The large β-decay energy suggests that many states can be fed in the β decay which deexcite via multi-γ-ray cascades to the ground state.

Since ^{76}Zn had not previously been studied using any transfer reactions, all the database information on the structure of ^{76}Zn comes from ^{76}Cu β decay [15]. The β decay of ^{76}Cu was first reported by Winger *et al.* [16] utilizing the high-resolution technique. They observed 12 γ rays associated with this decay, placing 11 γ rays into a decay scheme with 8 excited states up to 2974 keV. This experiment also suggested the presence of a β-decaying isomer due to an observed difference in the half-life measured using the 599- and 698-keV γ rays. Little could be decerned about collectivity from this measurement, and the proposed level scheme seemed to support a spherical shell model picture. The experiment was severely limited by the overwhelmingly strong ^{76}Zn component in the deposited source which made it difficult to identify the much weaker γ rays from ^{76}Cu decay. In a later study, Van Roosbroeck *et al.* [1] observed 15 γ rays and constructed a decay scheme with 9 excited states up to 3273 keV. They improved on the earlier experiment by using a laser ion source to selectively enhance ^{76}Cu over ^{76}Zn in their deposited source. As a result, they could avoid some of the pitfalls of the first experiment leading to a few corrections. First, they observed no evidence for an isomeric decay. Second, they saw no evidence to assign 4 γ rays to the decay, suggesting these were probably from ^{76}Zn or ^{76}Ga decays, and removed three levels. One major change was a switching of the order for a 464-1053-keV γ-ray cascade. In Winger *et al.*, an observed slightly higher intensity for the 464-keV γ ray suggested it be placed lower giving a level at 1761 keV, which would match with a spherical shell model picture. With Van Roosbroeck *et al.*, the intensities of the two γ rays were closer to being the same and they placed the 1053-keV γ ray lower, giving a state at 2349 keV which would indicate more collective behavior. In neither experiment was a crossover transition found to support the proposed placement. Finally, the highest observed energy level in ^{76}Zn fed in β decay was only 3273 keV, while $Q_{\beta-} = 11327(7)$ keV for this decay and $S_n = 7815.4(25)$ keV for ^{76}Zn [27] indicate a large window for feeding to higher-lying energy levels which were missed in the previous measurements. Thus the poorly known decay of ^{76}Cu and the structure of ^{76}Zn instigated our interest to revisit this decay. With a system which can produce ^{76}Cu at a higher rate while completely removing ^{76}Zn from our beam, along with a higher efficiency detector array, we expect to extend the existing decay scheme to significantly higher energies. Also, from the understanding of the recent work in Refs. [25,28], we intend to correct the placement for some of the γ rays and energy levels using the statistically significant $\gamma\gamma$ coincidence technique. Preliminary results from this study were presented in Ref. [29].

The study presented here significantly increases our understanding of levels in ^{76}Zn fed by the β decay of ^{76}Cu. Section II briefly describes the experimental setup and techniques employed for this study. Section III presents the results of the data analysis including the updated decay scheme. Finally, Sec. IV provides a comparison with shell model calculations along with a final discussion of the results.

II. EXPERIMENTAL TECHNIQUE

The experiment was performed at the Holifield Radioactive Beam Facility (HRIBF) in Oak Ridge National Laboratory (ORNL) at the same time as the two measurements described by Ilyushkin *et al.* [2,5]. A 54-MeV proton beam with an

intensity of 10–15 μA was used to bombard a uranium carbide (UC_x) target to produce fission fragments. The fission fragments were thermalized and passed into a hot-plasma ion source to produce positive ions which were extracted and accelerated to an energy of about 100 keV. Initial isobaric separation was achieved using the low-resolution mass separator ($M/\Delta M \approx 600$) to select the $A = 76$ nuclei. By passing the beam through a cesium-vapor charge-exchange cell, the ^{76}Zn ions which do not form negative ions could be removed from the beam using the subsequent high-resolution separator ($M/\Delta M \approx 10\,000$). Thus it was possible to separate the ^{76}Cu and ^{76}Ga components of the beam and provide a nearly pure beam of ^{76}Cu ions. By comparing the 599-keV γ ray from ^{76}Cu to the 563-keV γ ray from ^{76}Ga in the saturation spectrum, as described later, we are able to estimate the beam to be 83.9(22)% ^{76}Cu. The beam was sent to the Low-energy Radioactive Ion Beam Spectroscopy Station (LeRIBSS) where the ions were deposited onto a moving tape collector (MTC) in the center of the detector array. The LeRIBSS setup consists of four high-purity germanium (HPGe) clover γ-ray detectors and two plastic scintillation for β detection. The clover array has a measured peak efficiency of 29% at about 100 keV and 5% at 1.33 MeV. Data were collected using a triggerless digital data acquisition system which recorded the energy and absolute time (10 ns accuracy) [30,31] when any detector registered an event. This allowed offline analysis of the data to establish various γ-ray spectra as well as the $\gamma\gamma$ coincidence matrix. This experiment was designed as a followup to the ^{76}Cu β-delayed neutron emission experiment which has been previously reported [7].

In the experiment, data were collected using three different modes. First, with the MTC stationary, the beam was pulsed on for 3.8 s and off for 6.2 s, which enhances ^{76}Ga and ^{76}Zn relative to ^{76}Cu and provides good coincidence statistics for all members of the decay chain. This mode was run for 7.0 h. Second, a 5.0 s on, 1.2 s off MTC cycle, which enhances ^{76}Cu over its isobars, was run for 2.5 h. Finally, a saturation spectrum in which the MTC was stationary and the beam was not pulsed provides the best enhancement for ^{76}Zn over the other two modes; it was run for 1.6 h.

The absolute γ-ray photopeak efficiency (ϵ_γ) for the clover detectors in the configuration used for this experiment was measured using standard γ-ray sources of ^{133}Ba, ^{152}Eu, ^{137}Cs, ^{60}Co, and ^{226}Ra for an energy range from 53 to 2204 keV. In establishing the absolute photopeak efficiency, an estimated total γ-ray efficiency was determined based on a few data points to establish the ratio of total γ-ray efficiency to absolute photopeak efficiency, thereby allowing summing corrections to be performed. The summing corrections brought the calibration data points onto a smooth line, giving confidence in the total γ-ray efficiency curve even though it was not directly measured. As described in Tracy *et al.* [25], the absolute photopeak efficiency will have a linear behavior in a log-log plot for the energy range from 300 keV to 3 MeV, but shows a downward bend starting at $\approx$3.5 MeV. To extend the efficiency curve to energies above 3 MeV, we compared our efficiency curve below 3.5 MeV to other similar systems available in the literature [32–34]. By renormalizing these other efficiency curves, we obtained consistent values for the absolute photopeak efficiency in the 3 to 9 MeV range, allowing us to extrapolate the efficiency curve up to the 6 MeV range of our observed γ rays. The resulting data points were then fit to a six-term polynomial of $\log(\epsilon_\gamma)$ versus $\log(E_\gamma)$ to obtain the efficiency curve. The resulting efficiency curve was applied as described by Tracy *et al.* [25].

In the offline analysis, raw spectra from each crystal of the HPGe detectors were gain matched using strong background and $A = 76$ peaks of known energy and combined to generate both ungated and β-gated γ-ray singles spectra as well as several $\gamma\gamma$ coincidence matrices. In this process it was discovered that upper-end cutoff and pileup effects resulted in distortion of the individual spectra in the form of spurious peaks starting at $\approx$4.85 MeV. One detector was distortion free up to $\approx$5.40 MeV, allowing for extension of the energy calibration as described below. Finally, one crystal was distortion free, thus allowing observation of the highest energy γ rays reported here. The spurious peaks were clearly distinguishable from the local background and peaks, allowing them to be removed from the final spectrum shown in Fig. 2.

The ungated γ-ray singles spectrum generated from all the data (cumulative), shown in Fig. 2, was used to determine the centroids and areas of the observable peaks because of the energy dependency of the β detectors [2]. Fit parameters describing the skewed-Gaussian peak shape were determined from well-defined peaks and functions were fitted to describe these fit parameters as a function of energy (position). These fit parameters were then held fixed in the subsequent fitting of the γ-ray singles spectrum, which generated information on all observable γ-ray peaks in the spectrum. The exceptions are the peaks above 4.8 MeV, where the single detector and/or single crystal were analyzed and the area scaled to that of the full array. The distortion of the γ-ray spectrum is evident in Fig. 2 where the highest energy peak indicated [5284-keV single-escape peak (SEP) associated with the 5795-keV γ ray] is much weaker than the double-escape peak (DEP) at 4773 keV while they are expected to be of comparable peak area.

Although the γ-ray spectrum had been gain matched prior to analysis, an energy calibration of the spectrum was performed to determine the systematic uncertainty in the γ-ray energies. This calibration was performed up to 2.6 MeV using well known room background γ rays which were well separated from source γ rays. The calibration was then extended up to 5.4 MeV using escape peaks from various ^{76}Ga and ^{76}Cu γ rays identified in the spectrum. A listing of these γ rays is presented in Table I. The uncertainties in all the γ rays reported here include both the uncertainty in the peak centroids from the fitting procedure as well as the systematic uncertainty from the calibration fit.

All the γ-ray peaks seen in the ungated γ-ray singles spectrum should be associated with ^{76}Cu (and its βn daughters ^{75}Zn and ^{75}Ga), ^{76}Zn, ^{76}Ga, or room background. The background lines are well understood and are easily identified by comparing the ungated and β-gated spectra where they are completely removed. Assigning γ rays to the other decays involves several methods including comparison of the γ-ray singles spectrum from the various data collection modes (pulsed, MTC, and saturation), the coincidence information from the cumulative data, and the β-detection efficiency,

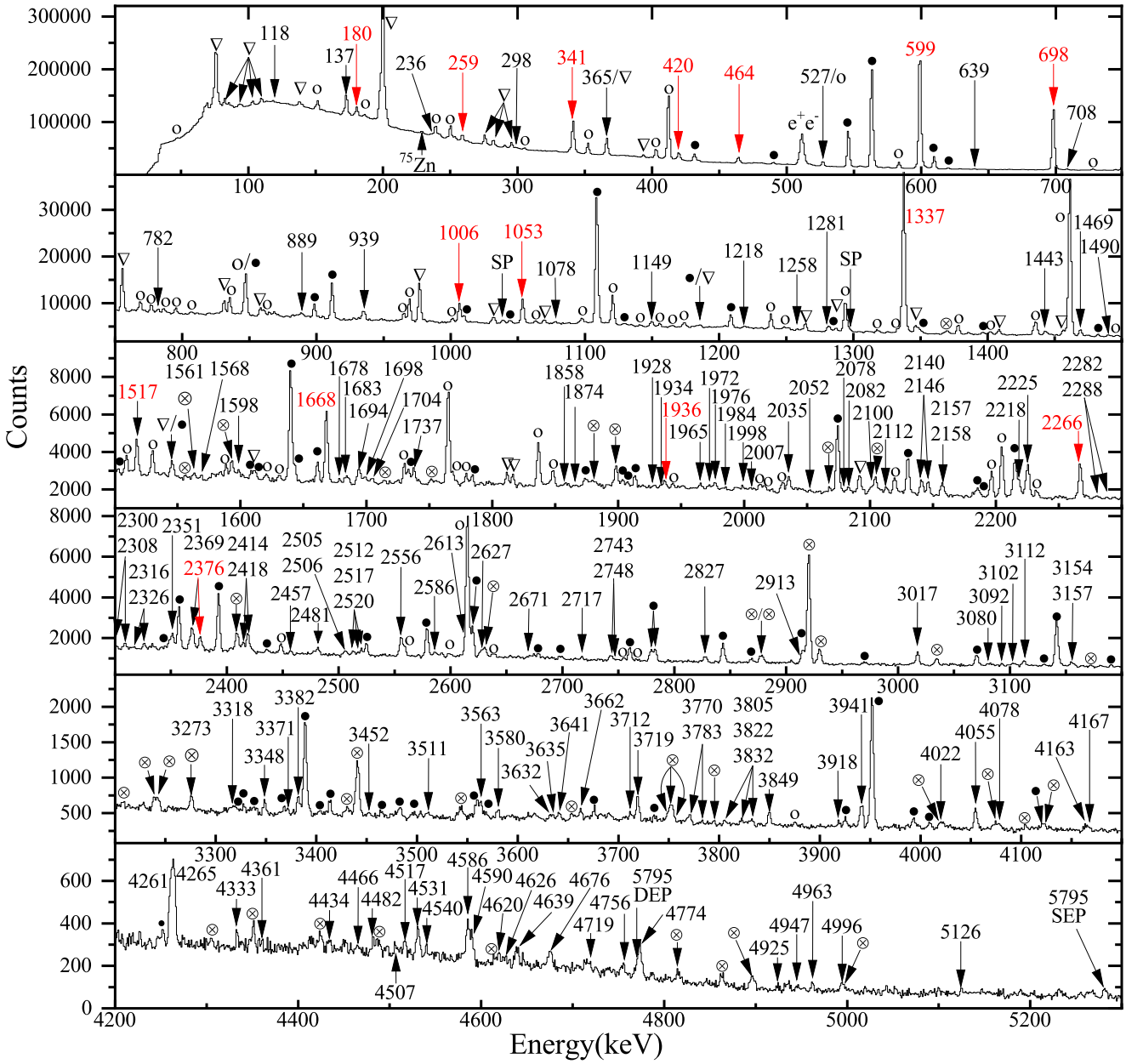

FIG. 2. Cumulative spectrum obtained in the LeRIBSS data run with a purified ^{76}Cu beam in the energy range from 20 keV to 5.3 MeV. The γ-ray peaks associated with ^{76}Cu decay are marked with their energy where those previously identified are marked in red. Peaks from other members of the decay chain are indicated by symbols as ^{76}Zn: ∇ (open down-triangle); ^{76}Ga: • (solid bullet); background: ○ (open bullet); and escape peak: ⊗ (crossed circle).

which depends mainly on the Q_β value for the decay. For example, the measured β efficiencies for the strongest γ ray in each $A = 76$ decay are 50.39(13)% for the 599-keV γ ray from ^{76}Cu, 28.93(9)% for the 200-keV γ ray from ^{76}Zn, and 25.26(10)% for the 563-keV γ ray from ^{76}Ga. Although each transition feeds the ground state in its decay, the values represent an average for the decay since they are fed by way of multiple transitions from higher-lying levels throughout their decay scheme. To obtain an idea of the range of β efficiencies for a decay, we can look at a two γ rays from the ^{76}Cu decay. First, the 419-keV γ ray, which depopulates a level at 3233 keV that appears to have significant direct feeding, has a β efficiency of 54.6(12)%. Second, the 2225-keV γ ray, which depopulates a level at 4859 keV that must be directly fed, has a β efficiency of 44.4(23)%. Hence, comparison of the relative intensities between the ungated and β-gated singles spectra can help to distinguish ^{76}Cu γ rays from those of the other decays. The second method uses comparison of the spectra from the three different MTC modes to separate ^{76}Zn from ^{76}Ga. Finally, the coincidence information can be used to confirm or show an assignment. By using these methods, 516 out of the 614 observed peaks were assigned to a source decay, to the background, or as an escape peak. The unassigned γ rays account for 3.8% of the total source intensity

TABLE I. Source γ rays used in the energy calibration where the energies were established using the observed energies of the escape peaks.

Source	Energy (keV)
^{76}Ga	2578.53(8)
^{76}Ga	2919.45(13)
^{76}Ga	3141.31(12)
^{76}Ga	3388.61(9)
^{76}Cu	3718.64(13)
^{76}Ga	3951.42(14)
^{76}Cu	4054.50(16)
^{76}Cu	4264.46(17)
^{76}Cu	4773.1(5)
^{76}Cu	5126.1(4)
^{76}Cu	5373.7(7)

(excludes identified background γ rays). The γ rays assigned to ^{76}Cu are indicated in Fig. 2 and listed in Table II, where the intensities are given relative to the 599-keV γ ray being 100%. The energies for all γ rays below 5.0 MeV are based on the position of the observed full energy peak, while above 5.0 MeV the energy uses the average derived from the SEP and DEP energies. This leads to a slight disagreement between the energies listed in Tables I and II for the calibration peaks.

In the past, most $\gamma\gamma$ coincidence analysis involved only a visual inspection of the background-subtracted coincidence spectrum to determine coincidences. However, in the simple qualitative visual inspection of the background subtracted spectra, it is not always clear which γ rays are in real coincidence or if an observed peak is just the residue from incorrect background subtraction. Another important issue to address was how to justify the placement of a γ ray to a new level if it was the only γ ray observed coming from the new level. To provide a quantitative answer to this question, we have developed a more objective plan by determining a statistical significance factor for each observed γ ray obtained from the projection of a $\gamma\gamma$ coincidence gate. Gaussian fits were performed for any peak observed in the peak gate to obtain an area and uncertainty $[A_P(\sigma_{A_P})]$, with care being taken to not include obvious backscatter peaks. The positions of these peaks were then fixed, and the same set of peaks were fitted in the background gate to obtain the area $[A_B(\sigma_{A_B})]$. The significance factor (S) was determined using

$$S = \frac{\Delta A}{\sigma} = \frac{A_P - A_B}{\sqrt{\sigma_{A_P}^2 + \sigma_{A_B}^2}}. \quad (1)$$

If a peak is found to have $S \geqslant 2.00$, i.e., 2σ above background, then the coincidence is considered to be possible, while if $S \geqslant 3.75$ (probability of 99.98%) it is considered a definite coincidence. This statistical significance factor provides the justification for the placement of γ rays to a new level as well as removing evaluator bias from the analysis. Typically, a regular $\gamma\gamma$ coincidence matrix was used. However, a coincidence matrix based on add-back spectra was also considered for low-energy γ rays where Compton backscatter peaks are large.

TABLE II. γ rays assigned to ^{76}Cu β decay indicating γ-ray energy (E_γ), relative intensity (I_γ), proposed deexcitation energy level, and $\gamma\gamma$ coincidence information. Probable coincidences are indicated with parentheses. The relative intensities presented were obtained after performing summing corrections based on the proposed decay scheme. For both energies and relative intensities, the uncertainties include both statistical and systematic factors.

E_γ (keV)	I_γ (%)	Level (keV)	$\gamma\gamma$ coincidences (keV)
117.88(13)[a]	0.30(4)	3273	137, (365), (3017)
137.47(5)[a]	1.12(5)	3155	118, (599), 2418, 3017
180.12(3)	3.21(11)	2814	420, 599, 698, 1337, (2035), 2146
235.81(11)[a]	0.48(4)		
258.63(3)	3.4(3)	3233	341, (527), 599, 698, (941), 1337, 2376
298.10(10)[a]	0.81(11)	3273	341, (365), (1337)
340.921(20)	19.5(4)	2975	259, 298, 599, 698, 782, 1149, 1337, 1694, (2035), (2520), 2743
365.47(24)[a,b]	1.39(18)	3638	599, 1006, (1668), 2267
419.499(20)	6.2(3)	3233	180, 464, 527, 599, 698, 1053, 1337, 1517, 1874, (2112)
464.160(22)	4.3(4)	2814	420, 599, 698, 1053, 2146
527.04(13)[a,c]	0.57(15)	3760	(259), (420), (599), 698, (1053)
598.706(14)	100.0(22)	599	137, 180, 259, (298), 341, 365, 420, 464, (527), (639), 698, (708), (782), (889), 1006, 1053, 1149, (1281), 1337, 1443, 1517, 1668, 1694, (1698), 1737, (1976), 2035, 2082, 2140, 2146, 2157, 2218, 2225, 2351, 2369, 2376, 2414, 2418, (2481), 2512, 2520, 2613, (2743), 2827, 2913, (3112), (3157), (3382), 3562, (3662), 3719, (3770), (3849), 3941, 4054, (4078), 4265, 4586, 4590, (4676), (4719), 4774, (4925)
639.08(14)[a]	0.36(5)	3273	(599), 698, 1337
697.815(14)	66.6(11)	1296	180, 259, (298), 341, (366), 420, 464, (527), 599, 639, 782, (939), 1053, 1149, (1281), 1337, 1443, (1469), 1517, 1678, 1694, 1737, (1976), (2112), 2146, 2218, 2225, 2369, 2414, (2512), (2520), (2586), (2671), (2743), 2827, 3563, 3662, (3831), 3849, 4054, (4078), 4265, (4590)
707.92(6)[a]	0.95(5)	2975	599, 1668, 2266
781.71(13)[a]	0.50(7)	3756	341, (599), 698, 1337

TABLE II. (*Continued*.)

E_γ (keV)	I_γ (%)	Level (keV)	$\gamma\gamma$ coincidences (keV)
888.59(11)[a,d]	0.57(5)	3155	(599), 1668, (2266)
939.1(5)[a]	0.14(6)	3573	(698), (1337)
1006.23(3)	2.95(7)	3273	365, 599, 1668, 2100, 2266
1053.22(3)	5.06(17)	2350	420, 464, (527), 599, 698, 2146, (2516)
1077.63(19)[a]	0.45(9)	4716	
1149.43(8)[a]	1.50(16)	4124	341, 599, 698, 1337
1218.47(22)[a]	0.50(22)	5887	
1258.0(3)[a]	0.24(5)		(599)
1280.98(9)[a]	1.44(9)	3915	(599), (698), 1337
1337.109(16)	38.3(7)	2634	180, 259, 341, 420, 599, (639), 698, 782, 939, (1149), (1281), 1469, (1490), (1598), 1694, (1873), 2082, 2225, (2326), 2369, (2512), 2520, 2586, 2743
1442.76(8)[a]	0.77(5)	2739	(599), 698
1468.9(3)[a,b]	0.67(14)	4103	(599), (698), (1337)
1489.85(18)[a]	0.33(5)	4124	(1337)
1517.38(4)	1.75(7)	2814	420, 599, 698, 2146
1561.2(5)[a]	0.39(5)	4716	
1568.3(3)[a]	0.22(5)		
1598.15(19)[a]	0.66(8)	4232	(599), (698), 1337
1608.14(18)[a]	0.49(6)		
1667.80(3)	4.65(9)	2266	(365), 599, (708), 889, 1006, 1965, (2157)
1678.3(4)[a,e]	0.000(0)	2975	(599), 698
1682.9(5)[a]	0.32(12)	4317	(1337)
1693.75(7)[a]	1.45(15)	4668	341, (698), 1337, 2376
1698.35(15)[a]	0.41(5)	4716	(599), 2418, 3017
1704.03(23)[a]	0.30(6)	4859	
1737.25(8)[a]	1.03(6)	3034	599, 698
1857.8(4)[a]	0.20(6)	3155	
1873.60(14)[a]	1.06(17)	5107	341, 420, 464, (698)
1907.0(3)[a]	0.33(6)		
1928.1(4)[a]	0.16(5)		
1933.5(6)[a]	0.15(5)	5146	
1936.49(18)	0.46(6)	3233	
1964.89(21)[a]	0.32(5)	4232	1668, (2266)
1971.8(3)[a]	0.38(9)	5887	
1976.35(16)[a]	0.50(6)	3273	(599)
1984.2(6)[a]	0.12(6)		
1998.4(3)[a]	0.27(6)		
2007.2(7)[a]	0.19(7)		
2034.74(14)[a,e]	0.025(5)	2634	341, 599
2051.8(4)[a]	0.22(6)		
2077.7(6)[a]	0.17(6)	5351	(1006)
2082.34(18)[a]	0.50(7)	4716	(599), (698), 1337
2100.29(20)[a]	0.54(7)	5373	(599), 1006, (1337), (1668)
2112.37(19)[a]	0.68(13)	5346	420, 599, (698)
2140.46(7)[a]	1.01(5)	2739	599
2145.64(8)[a]	1.41(9)	4959	180, (464), 599, 698, 1053, 1337, 1517

TABLE II. (*Continued*.)

E_γ (keV)	I_γ (%)	Level (keV)	$\gamma\gamma$ coincidences (keV)
2156.57(19)[a]	0.86(13)	4423	599, (1006), (1668)
2158.4(6)[a]	0.28(14)		
2217.85(9)[a]	1.36(7)	3514	599, 698
2224.91(9)[a]	3.19(24)	4859	599, 698, 1337
2266.38(4)	2.65(6)	2266	365, 708, 889, 1006
2281.6(7)[a]	0.17(7)		
2287.5(4)[a]	0.22(7)	5560	
2300.2(3)[a]	0.31(5)	5317	2418, (3017)
2308.38(18)[a]	0.50(6)	3605	(698)
2315.9(6)[a]	0.17(8)	5921	
2325.57(19)[a]	0.46(6)	4959	(599), 1337
2351.07(11)[a]	1.01(7)	2950	599
2368.91(21)[a]	1.27(16)	5003	599, 698, 1337
2375.80(8)	1.01(6)	2975	259, 599
2413.99(11)[a]	0.80(6)	3711	599, 698
2418.19(8)[a]	1.56(7)	3017	137, 599, 1698, 2300
2456.5(3)[a]	0.29(6)		
2480.91(14)[a]	0.49(4)	3080	(599)
2504.5(6)[a]	0.23(12)		
2506.4(6)[a]	0.23(11)	5523	
2512.43(19)[a]	0.44(6)	5146	(599), 698, 1337
2516.5(4)[a]	0.27(6)	4866	1053
2519.89(16)[a]	0.73(9)	5494	341, (599), (698), 1337
2555.62(19)[a]	0.37(9)	3155	(599)
2585.56(18)[a]	0.62(9)	5560	(341), (698), (1337)
2613.35(17)[a,c]	1.06(13)	3212	599
2626.75(19)[a]	0.58(7)		(599)
2670.6(3)[a]	0.23(5)	3967	698
2716.71(20)[a]	0.27(4)	4013	(599), (698)
2742.69(15)[a]	0.78(10)	5717	(341), 599, 698, 1337
2748.3(7)[a]	0.12(5)		
2826.95(15)[a]	0.63(5)	4124	(599), 698
2913.4(5)[a]	0.7(3)	3512	599
3016.81(9)[a]	1.17(5)	3017	118, 137, 1698, 2300
3080.0(6)[a]	0.21(6)		
3092.3(5)[a]	0.16(5)		
3101.5(7)[a]	0.24(9)		
3111.89(16)[a]	0.52(5)	3711	599
3154.1(3)[a]	0.46(8)		
3156.8(6)[a]	0.21(7)	3756	(599)
3272.7(5)[a]	0.15(6)		
3318.3(4)[a]	0.17(5)		
3348.16(19)[a]	0.40(5)		
3371.0(6)[a]	0.17(6)		
3381.61(15)[a]	0.63(5)	3980	599
3451.6(7)[a]	0.17(6)		
3510.9(5)[a]	0.12(4)		
3562.72(24)[a]	0.61(6)	4859	599, 698
3579.8(3)[a]	0.35(5)		
3631.7(9)[a]	0.16(7)		
3634.8(8)[a]	0.16(8)		
3640.6(3)[a]	0.33(6)		(698)
3662.10(21)[a]	0.48(7)	4959	(599), 698
3711.7(3)[a]	0.34(5)		(599)
3718.66(15)[a]	0.91(5)	4317	599
3770.0(3)[a]	0.31(4)	4369	599

TABLE II. (*Continued.*)

E_γ (keV)	I_γ (%)	Level (keV)	$\gamma\gamma$ coincidences (keV)
3782.7(8)[a]	0.11(4)		
3805.3(4)[a]	0.18(5)		
3822.0(4)[a]	0.22(4)		
3831.8(4)[a]	0.23(4)	5128	(698)
3849.46(19)[a]	0.58(5)	5146	599, 698
3918.3(3)[a]	0.12(3)		
3941.06(17)[a]	1.00(5)	4540	599
4022.3(8)[a]	0.20(8)		
4054.50(20)[a]	1.12(6)	5351	599, 698
4078.0(4)[a,d]	0.33(5)	5373	599, 698
4163.4(4)[a]	0.24(5)	5460	(698)
4166.8(5)[a]	0.19(5)		
4260.8(3)[a]	1.00(8)		
4264.59(25)[a]	1.35(8)	5560	599, 698
4333.2(3)[a]	0.20(4)		
4361.1(7)[a]	0.06(3)	4959	
4433.8(7)[a]	0.20(6)		
4465.6(9)[a]	0.14(5)		
4481.8(5)[a]	0.24(5)		
4507.0(7)[a]	0.13(4)		
4516.6(5)[a]	0.23(5)		
4531.3(3)[a]	0.53(5)		
4540.4(7)[a]	0.13(4)		
4585.7(4)[a]	0.68(5)	5184	599
4590.1(4)[a]	0.51(6)	5887	(599), (698)
4620.0(8)[a]	0.16(5)		
4625.7(7)[a]	0.14(4)	5921	(698)
4639.3(4)[a]	0.31(4)	5238	(599)
4675.8(5)[a]	0.51(6)	5973	
4719.0(6)[a]	0.12(3)	5317	(599)
4755.7(5)[a]	0.19(4)		
4773.6(5)[a]	0.49(6)	5373	(599)
4925.0(11)[a]	0.23(8)	5523	599
4946.7(10)[a]	0.23(10)		
4963.0(7)[a]	0.37(8)	5560	(599)
4995.7(6)[a]	0.61(11)		(698)
5126.1(6)[a]	0.22(7)	5725	(599)
5327.7(9)[a]	0.36(9)		
5375.4(7)[a]	0.52(8)	5973	(599)
5795.1(10)[a]	1.23(24)		
5921.0(11)[a]	1.26(25)		

[a]New γ-ray transition.
[b]Unresolved doublet with ^{76}Zn γ ray. Energy and intensity extracted from $\gamma\gamma$ coincidence data.
[c]Unresolved doublet with background γ ray. Energy and intensity extracted from $\gamma\gamma$ coincidence data.
[d]Energy is more than 2σ from that expected from the level-energy differences.
[e]Likely pure sum peak.

In some cases, the coincidence data indicate that an observed γ-ray peak was actually an unresolved doublet requiring two different placements. To determine the correct centroids and peak areas for the two unresolved γ rays, information from the $\gamma\gamma$ coincidence gates was used. The approximate centroids fitted within the coincidence-gated spectrum show slightly different positions for each member of the doublet. Whenever possible, the peak area was estimated by comparing to other γ rays either feeding or deexciting the same level using an appropriate gate [28]. A method was also developed to compare two γ-ray peak areas by gating on an intermediate transition in a three-member cascade. The analysis was done for each member of the doublet to check for consistency. This information was then used to refit the γ-ray singles spectrum to obtain refined values and uncertainties. For the ^{76}Cu, γ rays at 365 and 1469 keV were observed to be in unresolved doublets with ^{76}Zn γ rays. These are indicated in Table II.

III. EXPERIMENTAL RESULTS

Figure 2 shows the γ-ray singles spectrum from the full data set starting from a nearly pure ^{76}Cu beam. A total of 158 γ-ray peaks were associated with ^{76}Cu decay, which represents 40.2% of the identified source intensity in the analyzed spectrum. Table II contains a list of the ^{76}Cu γ rays indicating the γ ray energies, relative intensities, the level energies to which they are assigned, and the $\gamma\gamma$ coincidence information observed in our measurement. The coincidence information was determined using background subtracted γ-ray gated spectra utilizing the statistical test describe in the previous section. ^{76}Cu has a β-delayed neutron branch of 7.2(5)% [7,35], therefore we expected to and did observe some of the strongest γ rays from ^{75}Zn and ^{75}Ga β decay fed by the delayed-neutron branch. Van Roosbroeck *et al.* [1] in their work indicated that they did not observe any γ rays emitted by excited states in ^{75}Zn fed by the β-delayed neutron emission. We also do not observe any γ rays associated with emission from any excited state of ^{75}Zn [5]. We do observe a 1296-keV peak in the γ-ray singles spectrum as well as the coincidence spectra. Analysis shows that the area of the observed peak is consistent with it being a pure sum peak from the strong 698-599-keV cascade. In the β-gated spectrum, we identified γ-ray peaks at 527 and 2613 keV which are doublets associated with background peaks. We determined the centroids for these peaks from the β-gated spectrum, then used an approximate β-detection efficiency to estimate the peak areas used to determine their intensity reported in Table II. Other cases involving doublets were handled as described in the previous section. Based on the statistically significant $\gamma\gamma$ coincidence information in Table II, 92 γ rays were placed into the decay scheme for ^{76}Cu, shown in Figs. 3 and 4, containing 59 energy levels up to 6.0 MeV. An additional 13 γ rays were placed based on energy differences between established levels. In the decay scheme, levels established by multiple γ rays or a single γ ray which is observe in definite coincidence both ways are indicated by a solid line indicating strong confidence in the level. Those levels based on weaker coincidence information are more tentative, so the levels and associated transitions are indicated by dashed lines. The 25 transitions placed based on weaker coincidence information are indicated by dashed lines while the 13 transitions placed solely on an energy difference are indicated by dotted lines. After establishing the decay scheme, we performed summing corrections based on

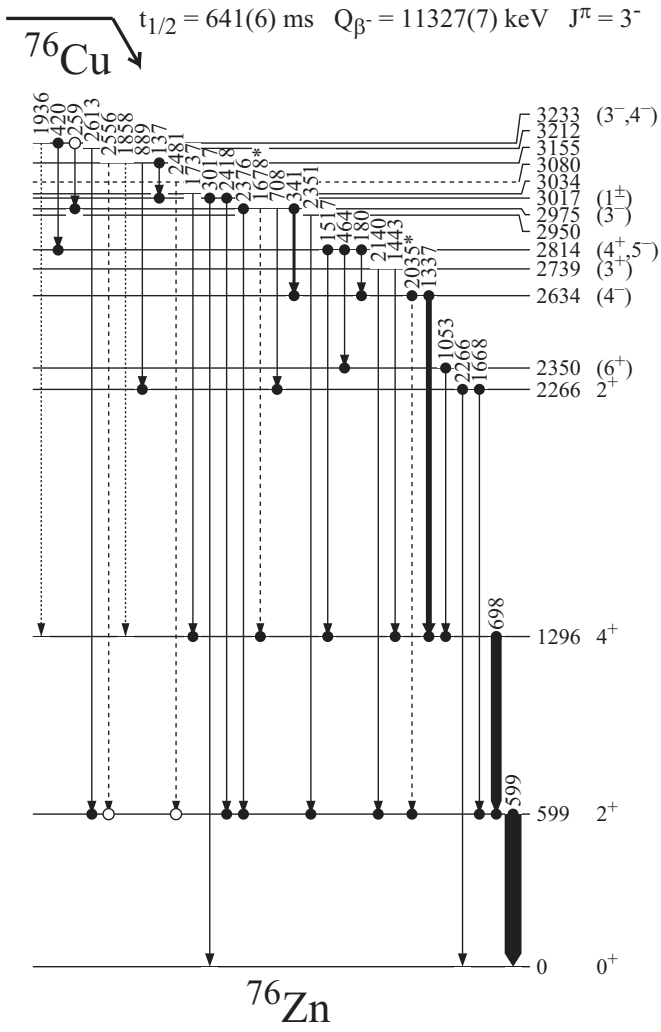

FIG. 3. Proposed decay scheme for ^{76}Cu to excited states in ^{76}Zn up to 3233 keV. Solid circles indicate definite $\gamma\gamma$ coincidences seen both ways, whereas open circles indicate probable coincidences. Transitions and levels without strong coincidence relationships are indicated by dashed lines. γ rays placed based solely on an energy difference are indicated by dotted lines. Also shown as dashed lines are the two transitions, flagged with a *, which may be pure sum peaks. The spin and parity assignments indicated are discussed in the text.

the level scheme to obtain the summing-corrected intensities given in the table. The placed transitions represent 95.2(8)% of our observed intensity associated with the decay of ^{76}Cu. The following sections will discuss specific results in more detail.

A. Is there an isomer?

As mentioned in the Introduction, a major difference between the earlier β-decay studies by Winger *et al.* [16] and Van Roosbroeck *et al.* [1] was the conjecture in the first experiment that a β-decaying isomer was present for ^{76}Cu, with a ground state half-life of 0.57(6) s and an isomer half-life of 1.27(30) s. The justification for the isomer proposed by Winger *et al.* was a difference in the apparent half-lives fit for the 599- and 698-keV γ rays as seen in Fig. 1 of that paper. Other Cu isotopes show isomers, so this was not a unexpected result. An experiment which measured β-delayed neutrons by Rudstam, Aleklett, and Sihver determined a single half-life of 641(6) ms [36], but this could have meant that the isomeric state did not decay to any states above the neutron separation energy. Van Roosbroeck *et al.*, however, did a comparison of the two γ rays (Fig. 6 in their paper) and saw no difference in the two half-lives. Since the same production method was used, any isomeric state should have been fed in both experiments. We repeated the comparison of the two γ rays with the results shown in Fig. 5. The two curves are identical, and the fitted half-lives are in agreement with Rudstam, Aleklett, and Sihver [36]. A possible explanation for the mistake made by Winger *et al.* is the presence of a γ-ray peak at 595.8 keV which has been tentatively assigned to ^{76}Zn β decay. Although much weaker in the current data set, this γ ray would have distorted the results of the earlier measurement where isobaric contaminants dominated the spectrum.

B. Modified decay scheme

Winger *et al.* [16] observed 12 γ rays associated with ^{76}Cu β decay and constructed a decay scheme with eight excitation levels up to 2974 keV. Their study used two HPGe detectors in 180° close geometry to record γ-ray singles and $\gamma\gamma$ coincidence information [16], but the source was dominated by isobaric contaminants. Van Roosbroeck *et al.* obtained a much cleaner production of ^{76}Cu by use of selective laser ionization. They utilized two HPGe detectors having a factor of 3 higher efficiency than the previous experiment and observed 15 γ rays associated with this decay, establishing a decay scheme with nine excitation levels up to 3273 keV [1]. Van Roosbroeck *et al.* observed eight of the γ rays reported by Winger *et al.*, but did not observe γ rays reported at 432, 1098, 1151, and 1783 keV. In our data set, the 432- and 1783-keV γ rays are assigned to ^{76}Ga β decay, as was also indicated by Van Roosbroeck *et al.* [1]. The former was previously reported by Camp and Foster [37], but showed a strong coincidence with a 599-keV γ ray. This suggests a weak γ ray from ^{76}Ga β decay near 599 keV. The 1783-keV γ ray was assigned due to a strong coincidence with the 432-keV γ ray. We do not observe this coincidence relationship, but do observe a definite coincidence with the 563-keV γ ray from ^{76}Ga β decay. Hence, there is no clear explanation for the original observation. We do not observe a 1098-keV peak in our β-gated singles spectrum as did Van Roosbroeck *et al.*, so its assignment based on energy in Winger *et al.* can be rejected. Finally, we do observe a γ ray at 1149 keV, as opposed to 1151 keV, but with a significantly lower relative intensity.

Van Roosbroeck *et al.* agreed with Winger *et al.* on placement for five levels while rejecting the levels at 1031, 1716, and 1761 keV. The 1031-keV level was proposed based on the 431-1783-keV coincidence and a good energy match to the well establish level at 2814 keV. There is no evidence for this cascade in the current data set. The 1716-keV level was proposed by placing the 419-keV transition as feeding the 1296-keV level. Both Van Roosbroeck *et al.* and the

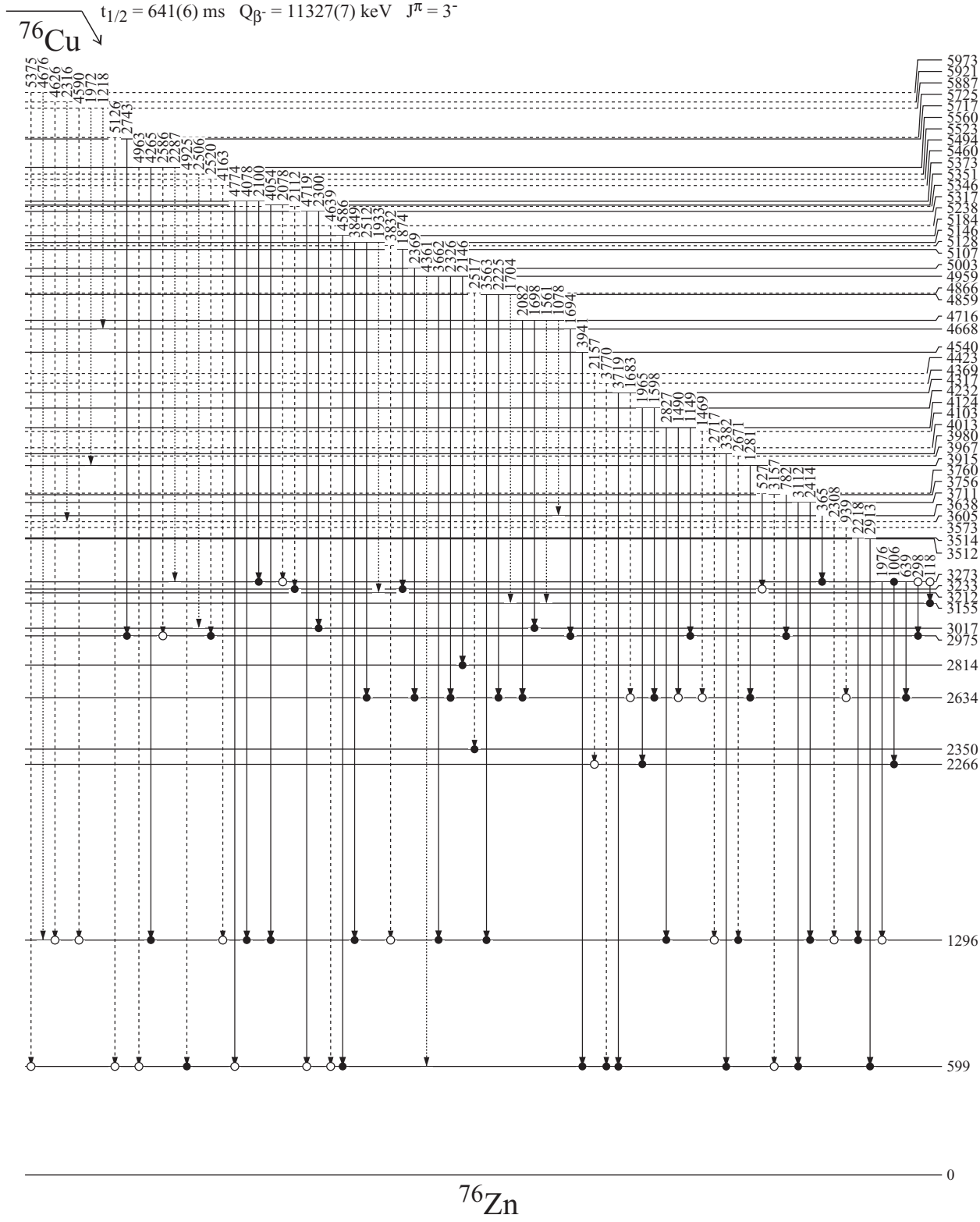

FIG. 4. Proposed decay scheme for ^{76}Cu to excited states in ^{76}Zn above 3233 keV. Solid circles indicate definite $\gamma\gamma$ coincidences seen both ways, whereas open circles indicate probable coincidences. Transitions and levels without strong coincidence relationships are indicated by dashed lines. γ rays placed based solely on an energy difference are indicated by dotted lines.

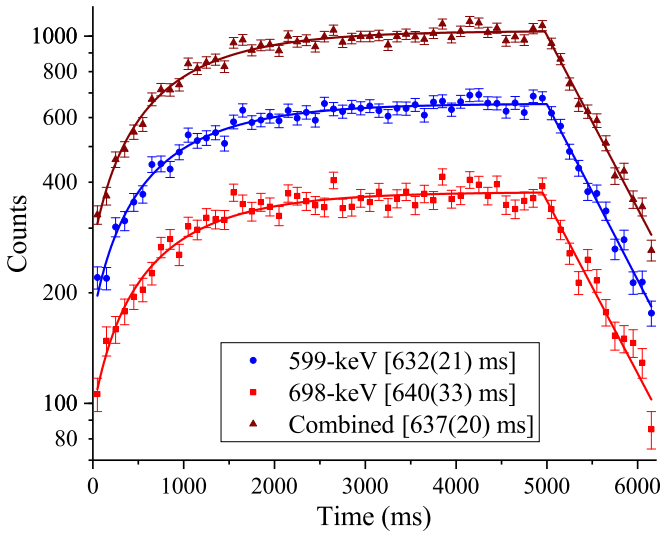

FIG. 5. Plot showing the half-life curves for the 599- and 698-keV γ rays and their combined data. Fitted lines for each data set are also shown with the determined half-lives in the legend. The results are consistent with the accepted value of 641(6) ms [36].

current work observe addition coincidences for the 419-keV γ ray indicating firm placement as feeding the 2814-keV level. Finally, as mentioned in the Introduction, Van Roosbroeck *et al.* removed the proposed level at 1716 keV by switching the order of the observed 464-1053-keV cascade connecting the 2814- and 1296-keV levels. In Winger *et al.*, the ordering of the cascade was based solely on the observed relative intensities of 2.9(7) and 2.4(10) for the 464- and 1053-keV γ rays, respectively, while Van Roosbroeck *et al.* observed relative intensities of 2.9(4) and 3.0(8), respectively, and placed the 1053-keV γ ray lower. In both cases the intensities are equal within measurement uncertainty and are consistent with no β-decay feeding to the intermediate level. Due to the ambiguity, both papers indicated the two transitions and the intermediate level with dashed lines. The only way to resolve the ambiguity is to observe a linking transition from the intermediate level to another level, i.e., a crossover transition. We searched our data set for such a transition. We do observe a 1751-keV γ ray which would link a level at 1760 keV to a newly proposed level at 3514 keV. A possible peak in a 464-keV gated coincidence spectrum is observed, but only for the add-back coincidence matrix, This observation can be explained as being due to summing of the 698- and 1053-keV γ rays. The β efficiency for this γ ray is too low to be due to ^{76}Cu decay, and a weak coincidence with the 545-keV γ ray indicates it is not the desired crossover transition. No other possible crossover transitions could be identified with either order for the cascade. Even the summing corrected intensities for the two γ rays are ambiguous since the larger intensity depends on the assumed order in the cascade. Hence, there is no justification purely from the data as to the proper order. Systematics for the Zn isotopes (Fig. 1 and Ref. [1]) tend to support a level at 2350 keV. There is now evidence that the 2350-keV level is the 6^+ yrast state which in β decay is fed from the 2814-keV level [38].

We propose a total of 29 new levels with firm coincidence evidence along with an additional 21 levels which are tentatively placed. Table III provides information on the proposed levels including energy, relative observed β-decay feeding intensity, and estimated $\log(ft)$ values based on the observed intensities. We have chosen to indicate firm placement of the 2350-keV level as well as the 464-1053-keV cascade due to the results of the high-spin experiment [38]. We agree with placement of all nine levels proposed by Van Roosbroeck *et al.* [1]. We have placed seven additional γ rays between the levels proposed by Van Roosbroeck *et al.*, but include the 1936-keV transition they proposed to feed the 1296-keV level as a dotted line. We observe a 1936.49(18)-keV γ ray which is in reasonable agreement with the energy difference between the levels [1936.75(4) keV]. However, the coincidence information is ambiguous. A 1936-keV gate using the add-back coincidence matrix shows strong coincidences with the 341- and 698-keV γ rays, but not the 1337-keV γ ray which would be expected if it were to feed the 2975-keV level as suggested by the coincidence with the 341-keV γ ray. Similarly, both the 341- and 698-keV gates show a peak at 1936 keV for the add-back coincidence matrix, but show no evidence for a peak in the normal coincidence matrix. The observed coincidence is due to a sum peak at 1935.8 keV from the 341-1337-698-598-keV cascade (598- and 1337-keV summed) that is much more pronounced in the add-back spectra. Evidence is much weaker in the normal coincidence matrix, and adjusting the peak and background gates can make the coincidence peaks go away. A simple estimate indicates that approximately half of the observed counts in the 1936-keV peak are due to the sum peak, so a real γ ray cannot be ruled out. Hence, the placement of the 1936-keV γ ray is based on the energy difference between established levels while the intensity is adjusted for the sum peak.

C. Level feedings

Understanding the decay of ^{76}Cu requires knowing the levels which are fed in β decay based on absolute intensities. The relative intensity of each γ ray can be converted into an absolute intensity by determining the normalization factor for the 599-keV reference peak. The normalization factor was not directly measured in this experiment since we did not count the number of ^{76}Cu ions deposited in the source, nor can the exact β-decay feeding to the ground state be determined. However, we can exclude direct ground-state feeding based on standard assumptions. The ground state spin-parity of ^{76}Cu has been experimentally measured to be 3^- [14]. Direct decay to the 0^+ ground state of ^{76}Zn would require a third forbidden transition which will not compete with allowed decays to negative parity states. Hence, it is safe to assume that direct feeding to the ground state is negligible and can be ignored. Therefore, within the β-decay branch, the total feeding will equal the sum of all the γ-ray intensity going to the ground state. Although β decay can feed 2^+ (first-forbidden) states, most decays will require at least a two γ-ray cascade to reach the ground state. Consequently, most of the unplaced γ rays in Table II would not go directly to the ground state and instead pass through the 599-keV level as is observed for the placed

TABLE III. Level energies, proposed spin-parity assignment, observed relative β-decay feeding intensities, and observed log(ft) values for ^{76}Zn from ^{76}Cu β decay.

Level energy (keV)	J^π	β-decay feeding (rel)	Observed log(ft) value
598.691(13)	2^+	15.0(25)	6.2
1296.488(19)	4^+	8.7(13)	6.3
2266.464(22)	2^+	1.65(20)	6.9
2349.65(3)	(6^+)	0.5(4)	7.4
2633.611(23)	(4^-)	5.7(9)	6.2
2739.20(6)	(3^+)	1.78(7)	6.7
2813.77(3)	$(4^+, 5^-)$	1.7(5)	6.7
2949.76(11)		1.01(7)	6.9
2974.54(3)	(3^-)	11.7(6)	5.8
3017.03(5)	(1^+)	0.65(16)	7.1
3033.74(8)		1.03(6)	6.9
3079.60(14)		0.49(4)	7.2
3154.60(5)		1.24(17)	6.8
3212.08(17)		0.91(14)	6.9
3233.23(3)	$(3^-, 4^-)$	7.8(5)	5.9
3272.69(3)		2.7(3)	6.4
3512.0(5)		0.7(3)	6.9
3514.34(9)		1.37(7)	6.6
3572.7(5)		0.14(6)	7.6
3604.92(18)		0.33(10)	7.2
3638.07(16)		0.95(20)	6.8
3710.51(10)		1.32(7)	6.6
3756.20(13)		0.71(10)	6.9
3760.27(13)		0.57(15)	6.9
3914.61(9)		1.06(13)	6.6
3967.1(3)		0.23(5)	7.3
3980.30(15)		0.63(5)	6.8
4013.20(20)		0.27(4)	7.2
4102.5(3)		0.67(14)	6.8
4123.81(7)		2.47(18)	6.2
4231.58(14)		0.98(9)	6.6
4317.28(14)		1.23(13)	6.5
4368.7(3)		0.31(4)	7.0
4423.03(19)		0.86(13)	6.6
4539.76(17)		1.00(5)	6.5
4668.27(8)		1.0(3)	6.5
4715.64(11)		1.74(13)	6.2
4858.60(8)		4.1(3)	5.8
4866.2(4)		0.27(6)	7.0
4959.30(7)		2.41(13)	6.0
5002.52(21)		1.28(16)	6.2
5106.83(15)		1.06(17)	6.3
5128.3(4)		0.23(4)	6.9
5145.97(13)		1.17(9)	6.2
5184.4(4)		0.68(5)	6.5
5237.9(4)		0.31(4)	6.8
5317.27(24)		0.42(6)	6.6
5345.60(19)		0.68(13)	6.4
5350.93(19)		1.30(9)	6.1
5373.15(17)		1.36(11)	6.1
5459.9(4)		0.24(5)	6.8
5494.43(16)		0.73(9)	6.3
5523.5(5)		0.46(14)	6.5
5560.47(14)		2.56(16)	5.8
5717.23(16)		0.78(10)	6.2
5724.8(6)		0.22(7)	6.8
5886.61(17)		1.4(3)	5.9
5921.3(5)		0.31(9)	6.6
5972.8(4)		1.03(10)	6.0

transitions. Therefore we will assume very few states will have transitions directly to the ground state, and that we have identified the majority of these transitions. The summed relative intensity to the ground state is then found to be 103.9(22). Given that $P_\beta = 92.8(5)\%$ [7], the normalization factor for the 599-keV γ is determined to be 0.893(19). Even if all the unplaced intensity feeds the ground state, the normalization factor only drops to 0.774(15).

The relative β-decay feeding intensities for each proposed level were determined from the difference between the summed γ-ray intensity observed feeding out of the level and the γ-ray intensity observed feeding into the level. These values are presented in Table III for the current study along with a comparison of the β-decay feeding profile for the three different studies shown in Fig. 6. From the figure, we can clearly see the shifting of β-decay feeding to higher energy levels as more detailed information became available. A comparison of β-decay feeding to major levels from the three studies is presented in Table IV. For the 599- and 698-keV levels, a significant reduction in the feeding is observed in the current study as a larger number of γ rays have been placed feeding into these levels. All levels below 3.0 MeV show this behavior. In contrast, the two levels above 3.0 MeV show an increase in feeding as more transitions are place deexciting the levels. Hence, feeding to the states below

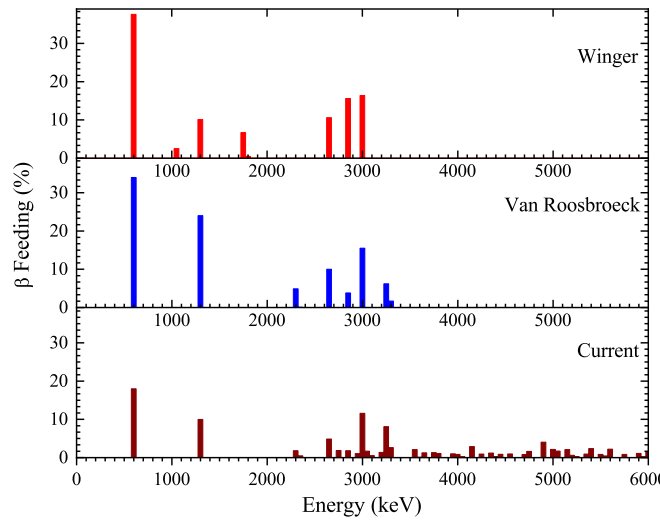

FIG. 6. Comparison of the β-decay feeding profile for ^{76}Cu β decay for the three experiments.

TABLE IV. Selected relative β-decay feeding intensities from each of the three measurements of ^{76}Cu β decay. See text for discussion.

E_{level} (keV)	Winger *et al.*	Van Roosbroeck *et al.*	Present work
599	47.(4)	38.(6)	15.0(25)
1296	20.(3)	23.3(25)	8.7(13)
2266		5.1(13)	1.65(20)
2634	11.(3)	10.2(23)	5.7(9)
2814	5.6(15)	4.0(7)	1.7(5)
2975	16.4(12)	16.(3)	11.7(6)
3233		6.4(12)	7.8(5)
3273		1.7(10)	2.7(3)

3.0 MeV probably represent upper limits while those above 3.0 MeV might be only lower limits. Finally, observed log(ft) values were determined utilizing the NNDC web site [39], with $Q_\beta = 11327(7)$ keV [27], $t_{1/2} = 641(6)$ ms [36], and the renormalized β-decay feeding intensities from Table III. Although log(ft) values provide no definitive information on the β decay to a certain level, large difference might be an indication of allowed versus first-forbidden decay.

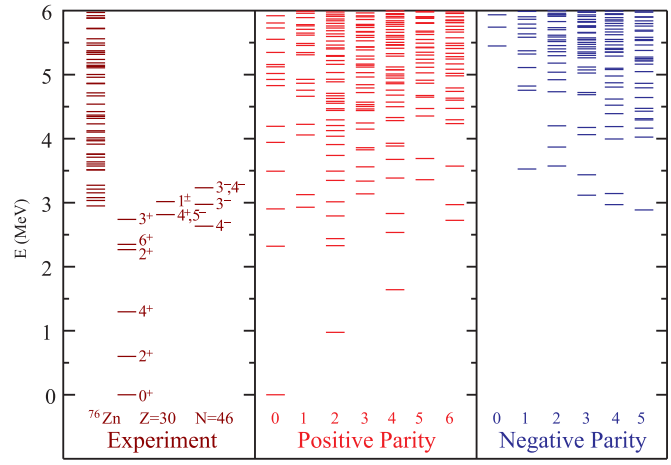

FIG. 7. Comparison of NUSHELLX shell model calculations for ^{76}Zn with our experimental work. The left column shows the experimentally identified levels with the positive and negative parity states separated from the continuum of unspecified states starting at $\approx$3 MeV. Results of the NUSHELLX calculations are shown for all states below 6 MeV with spins up to 6 for positive parity (center column) and spins up to 5 for negative parity (right column) states.

IV. DISCUSSION

A. Shell model calculations

We performed NUSHELLX [40] calculations using the jj44 model space with the JUN45 effective interaction [41] to provide a comparison to the experimental results and to give insight for spin-parity assignments. For ^{76}Cu, the shell-model calculation yields a 3^- ground state in agreement with the experimental measurement by Groote *et al.* [14]. The level structure of ^{76}Zn was calculated with no constraints for spins in the range $0 \leqslant J \leqslant 6$ with both positive and negative parity states for each spin and parity up to 9 MeV. Figure 7 shows a subset of the results for the levels obtained. The left-hand panel shows the experimental results where we have attempted to assign logical spin-parity values based on the experimental results as describe in the following section. The positive-parity states are shown in the middle column while the negative parity states are in the right-hand column. All other observed levels for which no spin-parity assignment is proposed are shown on the left side of the left-hand column. The 2_1^+ and 4_1^+ states clearly show that the results from the theoretical calculation are shifted up by $\approx$350 keV for these two states in comparison to the experimental results. This shift could be from several sources not contained in the model including evolution of the single-particle energies due to pairing and/or the monopole shift as well as the neglect of excitations across the $Z=28$ and $N=50$ shells. The truncation of the model space is likely the most significant effect as the addition of excitations across the shell gaps would lead to additional states mixing with those in the current model space with the result being lowering of the theoretical level energies to be more consistent with the experimental observation.

Based on the states determined in the calculation, various transition strengths were determined. First, the B(GT) strengths for the allowed β decays were determined. These will be compared to the observed β-decay feedings in Sec. IV C. Second, the $B(M1)$ and $B(E2)$ γ-ray transition strengths, along with the appropriate mixing ratios, were determined with states up to $\approx$3 MeV being considered. For these calculations, a standard set of parameters, including effective charges $e_p = 1.5e$ and $e_n = 0.5e$, was used [41]. $B(E1)$ transition strengths were not determined because we doubted the values would have any real meaning. This makes comparisons for the negative parity states difficult since an $E1$ transition will always be a possibility for decay out of these states. Nevertheless, a few negative parity states are including in the comparison. The results of the analysis are given in Table V and will be discussed in more detail in Sec. IV B. The values for the first two excited states are included for reference even though only a single transition would be observed out of each state. We do note that for all the cases presented that a single transition dominates the decay.

B. Spin and parity assignments

Having the information on the parent nuclei spin-parity, observed log(ft) values, theoretical transition strengths, and knowledge of level systematics, we have attempted to make tentative spin and parity assignments to the levels of ^{76}Zn. Winger *et al.* and Van Roosbroeck *et al.* both assigned 2^+ for the first excited state based on level systematics of $^{68-76}$Zn [1,16]. The β-decay transition from parent to daughter nuclei for this scenario is 3^- to 2^+ ($\Delta J = -1$ with parity change), which is a first-forbidden transition. Our lower-limit log(ft) > 6.1 for this level is in the accepted range (6.0–8.0), and would increase as more transitions are added feeding into the level.

The 1296-keV level only deexcites to the 2_1^+ state with no transition to the ground state. This observation limits the

TABLE V. Theoretical γ-ray transition strengths obtained in the NUSHELLX calculations for selected states with relative intensities greater that 0.05% presented. In the left five columns are the initial and final states involved along with the calculated level and γ-ray energies. The transition strengths and mixing ratios are given in the middle set of columns, while the predicted relative intensities for the transitions out of a state using the calculated energies are given in the ninth column. The last three columns present experimental results for the cases where we believe we have identified the corresponding experimental level. In some case the $E1$ transitions out of negative parity states suggested by the experimental results are included even though they were not part of the calculation. A more detail discussion of these results is given in Sec. IV B.

States		Theory energy			Transition strength			Relative	Observed experimental		
		Initial	Final	γ ray	$B(M1)$	$BB(E2)$		intensity	Energy	γ ray	intensity
Initial	Final	(keV)	(keV)	(keV)	(μ_N^2)	(e^2fm^4)	δ	(%)	(keV)	(keV)	(%)
2_1^+	0_1^+	967	0	967		156.60		100.00	599	599	100.0
4_1^+	2_1^+	1625	967	658		158.70		100.00	1296	698	100.0
2_2^+	0_1^+	2311	0	2311		3.54		3.08	2266	2266	36.3
	2_1^+		967	1344	0.190	161.80	−0.33	96.83		1668	63.7
	4_1^+		1625	686		44.16		0.09			
0_2^+	2_1^+	2316	967	1349		0.98		100.00			
2_3^+	0_1^+	2422	0	2422		9.19		2.66			
	2_1^+		967	1455	0.633	11.21	0.05	97.34			
4_2^+	2_1^+	2507	967	1540		27.01		3.74			
	4_1^+		1625	882	0.611	18.03	−0.04	96.26			
6_1^+	4_1^+	2730	1625	1105		106.10		99.98	2350	1053	100.0
2_4^+	0_1^+	2796	0	2796		1.07		4.90			
	2_1^+		967	1829	0.038	0.03	0.01	89.93			
	2_2^+		2311	485	0.043	0.10	0.01	1.87			
	0_2^+		2316	480		85.20		0.06			
	2_3^+		2412	384	0.149	0.89	−0.01	3.24			
4_3^+	2_1^+	2803	967	1836		11.45		1.27			
	4_1^+		1625	1178	0.790	0.25	−0.01	98.57			
	4_2^+		2507	296	0.078	18.32	−0.04	0.16			
1_1^+	2_1^+	2927	967	1960	0.571	0.46	0.01	97.62			
	2_2^+		2311	616	0.329	0.08	0.00	1.74			
	2_3^+		2422	505	0.199	0.22	0.00	0.58			
4_1^-	5_1^-	2932	2861	71	0.002	178.50	−0.16	100.00	2634		
	4_1^+									1337	100.0
3_1^-	5_1^-	3076	2861	215		18.63		0.10	2975		
	4_1^-		2932	144	0.198	50.55	−0.02	99.90		341	95.4
	2_2^+									708	4.6
1_2^+	0_1^+	3096	0	3096	0.254	0.00	0.00	87.91			
	2_1^+		967	2129	0.066	23.10	−0.33	8.24			
	2_2^+		2311	785	0.497	17.55	0.04	2.81			
4_2^-	5_1^-	3112	2861	251	0.213	0.69	0.00	92.31			
	4_1^-		2932	180	0.048	18.58	0.03	7.60			
	3_1^-		3076	36	0.063	119.30	−0.10	0.08			
3_1^+	2_1^+	3126	967	2159	0.088	1.28	0.07	27.25	2739	2140	56.7
	4_1^+		1625	1501	0.690	0.60	−0.01	71.23		1443	43.3
	2_2^+		2311	815	0.011	0.59	0.05	0.19			
	2_3^+		2422	704	0.031	28.48	−0.18	0.34			
	4_2^+		2507	619	0.072	0.82	0.02	0.52			
	2_4^+		2796	330	0.365	19.82	0.02	0.40			
	4_3^+		2803	323	0.060	1.54	0.01	0.06			

spin-parity assignment to be 0^+, 2^-, $3^\pm$, or 4^+. Systematics of the Zn isotope (Fig. 1) favor the 4^+ assignment unless the 0^+ state drops in energy beyond $A = 74$; however, the shell model calculations (Table V) have this state continuing the upward trend. Similarly, no odd spin or negative parity states are predicted in the NUSHELLX calculation at this low energy. Van Roosbroeck *et al.* argues that most of the levels above 2266 keV deexcite by one or more steps into the 1296-keV level and not to the ground state or 599-keV level, indicating that these higher-lying levels have a spin greater than 2, and effectively rules out the 0^+ assignment [1]. Although we observe additional feeding to the 599-keV level, the observed feeding into the 1296-keV level is a factor of 2.5 higher. Winger *et al.* [16] proposed the 1296-keV level to be the 4_1^+ state based on the strong $341 \rightarrow 1337 \rightarrow 698 \rightarrow 599$-keV γ-ray cascade, a feature which had been seen in the β decay of the high-spin isomers of ^{68,70}Cu [42,43]. We therefore assign the level as the 4_1^+ state, in which case the β decay is again a first-forbidden transition with the observed $\log(ft) > 6.3$ being consistent.

The 2266-keV level shows transitions to the ground and first excited states, but no transition to the 1296-keV level is observed. This observation tends to limit the spin-parity assignment to $1^\pm$, although a 2^+ state is not disallowed if deexcitation to the 4_1^+ state is prohibited due to structure reasons. The NUSHELLX calculations (Table V) indeed indicate negligible feeding to the 4_1^+ state; however, the prediction favors a strong $M1$ dominated transition to the 2_1^+ state with much weaker feeding to the ground state. The calculations also indicate the first spin 1 states should lie closer to 3 MeV, effectively ruling out this option. Systematics for the Zn isotopes (Fig. 1) suggest the 2_2^+ state to lie near 2 MeV. As seen in Table V, the observed relative intensities of the transitions to the ground and first excited states are 36.3% and 63.7%, respectively. This is similar to what is observed for the assigned 2_2^+ states in ^{70}Zn (41:59) [43], ^{72}Zn (40:60) [44], and ^{74}Zn (33:67) [25]. Consequently, we assign this as the 2_2^+ state with the observed $\log(ft) > 6.9$ being consistent with a first-forbidden β decay.

The 2634- and 2975-keV levels, each of which serves as a major path for the deexcitation of higher-lying presumably negative-parity states fed by allowed β decay, show a significant increase in apparent β-decay feeding over the nearby levels. The $\log(ft)$ values are lower, but not strongly indicative of allowed β decays. In fact, it is apparent (see Table III) that the β-decay intensity is being spread across a large number of states with none showing a low $\log(ft)$ value. The 2634-keV level deexcites to the 2_1^+ and 4_1^+ states, although the weak intensity of the 2035-keV transition cannot rule it out as a sum peak. In contrast, the 2975-keV level deexcites to the 2_1^+, 2_2^+, and 2634-keV states where the strongest transition de-excites to the 2634-keV level. These observations are consistent with a 3^- assignment for either state. However, the NUSHELLX calculations (see Table V) indicate that both the 4_2^+ and 4_3^+ states will decay primarily to the 4_1^+ state, so a 4^+ assignment for the 2634-keV level cannot be rejected if the β feeding is actually lower due to missing feeding transitions. What is interesting for these two states is the $341 \rightarrow 1337 \rightarrow 698 \rightarrow 599$-keV γ-ray cascade which establishes these levels. A similar structure is seen in the β decays of ^{68,70}Cu [42,43], but not for ^{72,74}Cu [25,44] where the β-decaying state has a lower spin. For ^{68}Cu decay, the 6^- isomer feeds a $(6)^-$ state which decays though a well established $6_1^- \rightarrow 5_1^- \rightarrow 4_1^+ \rightarrow 2_1^+ \rightarrow 0_1^+$ cascade, while for ^{70}Cu the 3^- isomer feeds the cascade starting with a $(3^-, 4^\pm)$ state. Van Roosbroeck *et al.* favored 4^- while the NNDC proposed other options [15,43]. The Van Roosbroeck *et al.* assignment can be rejected, as pointed out by the NNDC evaluators, since the strongest transition is to a (2^+) state. Similarly, the (4^+) assignment can be rejected due to an apparent allowed β decay to the state. Therefore, the 3247-keV level in ^{70}Zn is most likely the 3_2^- state. Although the progenitor state for the cascade differs, the lower portion remains the same suggesting our 2634-keV level could be the 5_1^- state. This also agrees with the NUSHELLX calculations which place the 5_1^- as the lowest negative parity state just below 3 MeV. In the $N = 46$ isotone ^{78}Ge, the lowest 5^- state is observed at 2646 keV and decays to the two lower-lying 4^+ states [45]. A 5^- assignment for the 2634-keV level would require the apparent β-decay feeding to be due to unobserved γ-ray intensity feeding into the state, while the 2035-keV γ ray would need to be a pure sum peak, something which could not be proved within the current data set. Our NUSHELLX calculations suggest a $3^- \rightarrow 4^- \rightarrow 5^-$ cascade; however, shifting the order of the lower two states, which are very close in energy, would break the cascade. The 2975-keV level could be explained by a low-energy $E1$ transition competing with higher-energy $E2$ transitions to the 2^+ states, which would then favor a 4^+ assignment. However, the NUSHELLX calculations do not indicate that any 4^+ states would give equal feeding to the 2_1^+ and 2_2^+ states. An alternative explanation in line with observed cascades in nearby nuclei is possible. In ^{70}Zn, the first 3^- state, which is at lower energy than the first 5^- state, has transitions to the lower-lying 2^+ and 4^+ states. If the 4_1^- or 5_1^- state is pushed lower in energy, then decays from the 3_1^- state to positive or negative parity states would be possible. The NUSHELLX calculations indicate that β feeding to the 3_1^- and 4_2^- states is approximately twice that of the feeding to the 4_1^- state, which is approximately what is observed for the 2634- and 2975-keV levels. Based on this evidence, we favor a 3^- assignment for the 2975-keV level and 4^- for the 2634-keV level, although 5^- for the later case cannot be rule out.

The 2739-keV level deexcites to the 2_1^+ and 4_1^+ levels. However, there is no indication of enhanced feeding in the β decay even though no transitions were identified to enter the state. Therefore, there is no strong evidence for it being a negative parity state. A 2^+ or 4^+ state is consistent with the NUSHELLX calculations which show the 2_3^+ and 4_2^+ states at nearly the same energy. However, neither of these states indicate similar transition intensities to the lower states. In fact, all the predicted 2^+ states near this energy show a strong transition to the 2_1^+ state with no feeding to the 4_1^+ state. Similarly, the 4^+ states indicate a strong transition to the 4_1^+ state with a much weaker transition to the 2_1^+ state. An alternative explanation would be the 3_1^+ state which does show a more reasonable intensity pattern, but which is predicted to be at a much higher energy. Nevertheless, we favor the 3^+ assignment to this level based on the splitting of intensity.

As mentioned previously, the 2350-keV level is proposed as the 6_1^+ member of the yrast band [38], but we cannot rule out a 4^+ assignment since the NUSHELLX 4^+ states near this energy have a dominant transition to the 4_1^+ state. However, the energy in consistent with the yrast states being lowered in energy by ≈350 keV. This level has essentially zero observed β-decay feeding, and is only observed to be fed by the single 464-keV transition from the 2814-keV level. The 2814-keV level also deexcites to the 4_1^+ level as well as the lowest proposed negative parity state at 2634 keV. The 180-keV transition would need to be of lower multipolarity in order to compete with the other two transitions, which is consistent with the observed decay pattern if the 180-keV transition is $E1$ while the other two are at least $M1$. These considerations limit the spin-parity for the 2814-keV level to 4^+, 5^+, and 6^+. The NUSHELLX calculations suggest multiple 4^+ states lower than the first 5^+ state, and it seems unlikely that a 6^+ state would be a deexcitation path for the negative parity states with spins less than 4 which are fed by the β decay. The transition strengths obtained in the NUSHELLX calculations (Table V) do not provide much clarification since the 4_2^+, 4_3^+, and 4_4^+ states all show a single dominant (>95%) transition to the 4_1^+ state. The calculations place the 4_2^+ state below the 6_1^+ state with a $B(E2) = 67.53\ e^2\,\mathrm{fm}^4$; however, reversing the order of the levels and adjusting for the observed energies, the intensity of the $4_2^+ \rightarrow 6_1^+$ transition is negligible. Alternatively, the 2814-keV level could be a 5^- state, for which the $E1$ transition to the 2350-keV level is preferred. Consequently, we have indicated a spin-parity assignment of 4^+ or 5^- for the 2814-keV level. The question is then, why do we observe the spin up to the 6^+ state? A similar situation occurs in the β decay of ^{70}Cu [43], where the decay of the 3^- isomer leads through the probable 5^- state. Hence, the structure of the states must be favorable to enhance the decay path going through a higher-spin state.

The 2950-keV level along with several others is established by a single transition to the 599-keV level with no observed transitions feeding the state. Although the states have apparent feeding, the $\log(ft)$ values are more consistent with a first-forbidden decay. If they are fed by allowed decays, then the spin and parity would be limited to 2^- and 3^-. However, the negative parity states in the NUSHELLX calculations tend to be at higher energies even after shifting them down as proposed earlier. It is possible that they are positive parity states fed by multiple $E1$ transitions which are not observed in this experiment. Similarly, there are a number of states, for example the 3034-keV state, which are only connected to the 1296-keV level and for which the same set a arguments can be made. Consequently, no reasonable guess at an assignment can be made for these states.

The 3017-keV level connects to the first excited (57.1%) and ground (42.9%) states by transitions of similar intensity, has low apparent β-decay feeding, and is fed by states which are likely fed by allowed β decay. Hence, $1^\pm$ or 2^+ are the most likely assignments. Although the $\log(ft)$ value (7.1) is low for a first-forbidden unique (1^+) or second-forbidden (2^-) β decay, unobserved γ-ray feeding into the state could easily increase the $\log(ft)$ value to be consistent with these decay modes. A 1^- assignment is possible in this case, where the NUSHELLX calculations do give a possible state if it is shifted down in energy as is seen with the yrast and 4_1^- states. There are two 1^+ states in the calculation near this energy, while multiple 2^+ states are predicted. Since the intensities of the two transitions out of the state are approximately equal, we would assume the same multipolarity for both. All the predicated 2^+ states in this energy region (Table V) show a dominant transition to the 2_1^+ state with only a small branch to the ground state. The calculated branching ratios for the 1_1^+ state indicate that a single transition to the 2_1^+ state dominates with no branch to the ground state, while the 1_2^+ state has these reversed. If the actual state is more mixed than predicted, a 1^+ assignment would be justified. However, the lack of a single positive parity state with the observed branching ratios provides support for the 1^- assignment where decay to the 3_1^- state is hindered by the small energy difference, while the $E1$ transitions to the first two states are observed. We chose to reject the 2^+ assignment due to the multipolarity argument and the NUSHELLX predicted branching ratios. Therefore, $1^\pm$ is most likely, but no firm assignment can be made.

The levels at 3155 and 3273 keV have interesting decay patterns where transitions with lower energies complete with higher-energy transitions along with significant apparent β-decay feeding. It is unlikely that all transitions out of these states would have the same multipolarity, but instead $E1$ transitions are favored for the lowest energy γ rays deexciting each level. This makes sense for the 3273-keV level where a 2^+ assignment would reasonably match the observed decay pattern. However, this assignment favors a negative parity for the level at 3155 keV, which is inconsistent with its decay pattern. Consequently, no logically justified assignment can be made for these levels at this time.

The level at 3233 keV has significant apparent β-decay feeding with deexciting transitions to proposed 3^- and 4^+ states. These observations would favor a 3^- or 4^- assignment for the state. However, the 259- and 419-keV γ rays have similar intensity which would not be consistent with $M1$ and $E1$ transitions, respectively, unless there is a structural reason for having the 259-keV transition favored over the 419-keV transition. A major structural difference would be needed to explain why the 1936-keV transition, an $E1$ transition if the 3233-keV level is negative parity, is much weaker. An alternative explanation is a 2^+ assignment which favors an $E1$ transition for the 259-keV transition and a $E2$ transition for the other two cases where the 419-keV transition is favored for structural reasons. However, the significant apparent β-decay feeding rules out this assignment. The β-feeding calculations indicate the 3_2^- state has a feeding of less than half the feeding to the 3_1^- and 4_2^- states, which would support an assignment of 4^- for the 3233-keV level with the previously mentioned 3273-keV state being the more weakly fed 3^- state. However, assignment of the 3273-keV level remains tenuous and we indicate the assignment as 3^- or 4^- for the 3233-keV level.

It is difficult to make spin-parity assignments to the states above 3.5 MeV due to a lack transitions as well as confusing decay patterns. Of those states for which we have identified multiple deexciting transitions, most decay to both positive and negative parity states. In these cases, an $E1$ and a $M1$ transition must compete meaning that the lower-energy

transition is probably $E1$. Since the state fed by the suspected $E1$ transition is proposed to be a negative parity state, the deexciting level would be positive parity in contradiction to the expectation of the states being negative parity and directly fed by allowed β decay. Consequently, no further spin-parity assignments are suggested.

C. β-decay profile

As mentioned in the Introduction, one aspect of the measurement was to understand the limitations in a high-resolution study for determining the complete β-decay profile. It is obvious from Fig. 6 that the current study represents a significant increase in mapping out the β-decay profile. However, the highest energy level observed in this study represents only 76% of the available energy window up to the neutron separation energy ($S_n = 7815.4(25)$ keV [27]). A significant β-delayed neutron branch exists $P_{\beta n} = 7.2(5)\%$ [7], so it is expected that the 2 MeV range above the highest observed state and S_n should be filled with levels. In addition, only 67% of the observed γ rays associated with the decay could be placed in the decay scheme. However, the unplaced γ rays represent only 4.2% of the total assigned intensity with an average relative intensity of 0.26%. Obtaining viable coincidence statistics on the unplaced γ rays will require not only an order of magnitude or higher statistics, but will also increase the number of observed γ rays. This is certainly a good example of pandemonium with a large number of weak transitions from the nearly uniform distribution of predicted states shown in Fig. 7. Consequently, a high-resolution study has little hope for a complete mapping of the β-decay profile.

To quantify this expectation, we have compared the results of B(GT) calculations for allowed β decays from ^{76}Cu to ^{76}Zn determined in our shell model calculations to our measured level feedings. To provide a direct comparison, we have converted the B(GT) values from the calculation to expected β-decay feedings using

$$I_\beta = \frac{t_{1/2}}{K\left(\frac{g_V}{g_A}\right)^2} B(\mathrm{GT}) f(Q-E), \tag{2}$$

where $K = 6143.6(17)$ s, $g_V/g_A = -1.270(3)$, $t_{1/2} = 641(6)$ ms [36], $Q = 711.327(7)$ MeV [27], and E is the excitation energy. The Fermi integral $f(Q-E)$ was extracted using a simple three-parameter polynomial fit to tabulated values to allow for an easier conversion. The theoretical B(GT) values were summed into 100 keV bins and the Fermi integral was determined for the midpoint energy of this bin. After converting the B(GT) values using Eq. (2), the values were normalized to sum to 100%. The experimental data were summed into the same 100 keV bins as the theoretical values. The result is shown in Fig. 8. First, note that the predicted feeding profile provides a reasonable but slightly low estimate of 1.70% for the β-delayed neutron branch. A slight shift of the states just below the neutron separation energy would account for the difference between the theoretical and experimental results. Second, note that the energies of the lowest fed negative parity states may be shifted lower by a few hundred keV, but that most of the states below 3 MeV are positive parity states that can be fed by first-forbidden β decay. Third, what is abundantly clear is that the majority of the allowed feeding between 5.5 and 7.8 MeV (≈65%) was not observed in this experiment. Consequently, much of the intensity which feeds through the 599- and 1298-keV levels has yet to be identified and the apparent feeding to the states near 3 MeV may be overestimated. Although both allowed and first-forbidden decays can occur, a significant portion of the allowed decays are missed while the first-forbidden decays are significantly overestimated.

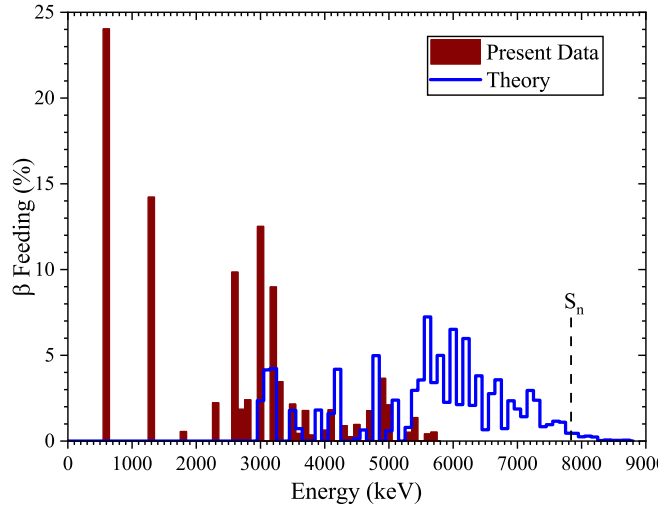

FIG. 8. Comparison of NUSHELLX shell model calculations for energy level feedings in the decay of ^{76}Cu to ^{76}Zn with our experimental work. The neutron separation energy ($S_n = 7.8154(25)$ MeV) for ^{76}Zn is shown as a vertical dashed line. See text for details.

It is apparent from this experiment that obtaining a full accounting of the γ-ray transitions and level feedings in a high-resolution measurement for cases with a large decay energy window will be nearly impossible due to the large number of weak transitions involved. Even with a much higher efficiency detector array, the ability to place hundreds of γ rays in a decay scheme would be a immense task with little gained benefit. In contrast, a total absorption spectroscopy measurement with much lower resolution can measure the complete β-decay profile, but with less knowledge of the actual states involved. The advantage then of the high-resolution studies is to identify individual states up to the energy where the continuum of states begins which are either strongly fed due to a favorable overlap of the wave functions between the parent and daughter states, or are significant pass-through states in cascades to the ground state.

V. CONCLUSION

Starting with a very pure beam of ^{76}Cu, a high resolution β-decay study was performed. We have identified 158 γ rays associated with this decay which is over 10× more than are currently listed in the NNDC database [15]. We have extensively increased the decay scheme with the addition of 144 previously unidentified γ rays, used statistically significant

$\gamma\gamma$ coincidences information to propose 50 new levels up to 5973 keV involving 91 new transitions. We introduced a technique to determine energies and intensities for unresolved doublets. Our proposed decay scheme represents 76% of the β-decay energy window which along with the known β-delayed neutron branch and 53 unplaced γ rays indicates that a significant portion of the β-decay profile is missing. Completing the β-decay profile will require a total absorption spectroscopy measurement.

Note added in proof. Two papers were published during the review process for this manuscript. Reference [46] measured the half-life of the 2634-keV level to be 25.4(4) ns indicating a negative parity state with a slight preference toward a 6^- assignment. Therefore, determining if the observed 2035-keV transition is a pure sum peak is extremely important. Reference [47] in a precision mass measurement did observe an isomeric state at 64 keV which could feed higher-spin negative parity states, helping to provide a pathway to the 6^+ and 6^- states. The Fig. 5 shows no indication of a second half-life, therefore the isomer may have a half-life very similar to that of the ground state.

ACKNOWLEDGMENTS

We would like to acknowledge the Holifield Radioactive Ion Beam Facility (HRIBF) and their staff for assistance during the experiment. The authors would like to acknowledge useful discussions with W. B. Walters and J. H. Hamilton. This research is supported by the Office of Science, U.S. Department of Energy under Grants No. DE-SC00-144448, No. DE-FG02-96ER41009, No. DE-FG02-96ER40983, No. DE-AC05-00OR22725, DE-FG02-96ER40978, No. DE-FG05-88ER40407, and No. DE-SC0016988; by the National Nuclear Security Administration under the Stewardship Science Academic Alliances program through DOE Cooperative Agreement No. DE-FG52-08NA28552; and by the Foundation for Polish Science.

[1] J. Van Roosbroeck, H. DeWitte, M. Gorska, M. Huyse, K. Kruglov, D. Pauwels *et al.*, Phys. Rev. C **71**, 054307 (2005).
[2] S. V. Ilyushkin, J. A. Winger, C. J. Gross, K. P. Rykaczewski, J. C. Batchelder, L. Cartegni *et al.*, Phys. Rev. C **80**, 054304 (2009).
[3] J. A. Winger, K. P. Rykaczewski, C. J. Gross, R. Grzywacz, J. C. Batchelder, C. Goodin *et al.*, Phys. Rev. C **81**, 044303 (2010).
[4] K. T. Flanagan, P. Vingerhoets, M. L. Bissell, K. Blaum, B. A. Brown, B. Cheal *et al.*, Phys. Rev. C **82**, 041302(R) (2010).
[5] S. V. Ilyushkin, J. A. Winger, K. P. Rykaczewski, C. J. Gross, J. C. Batchelder, L. Cartegni *et al.*, Phys. Rev. C **83**, 014322 (2011).
[6] A. Korgul, K. P. Rykaczewski, R. K. Grzywacz, C. R. Bingham, N. T. Brewer, C. J. Gross *et al.*, Phys. Rev. C **95**, 044305 (2017).
[7] J. A. Winger, S. V. Ilyushkin, K. P. Rykaczewski, C. J. Gross, J. C. Batchelder, C. Goodin *et al.*, Phys. Rev. Lett. **102**, 142502 (2009).
[8] E. Mané, B. Cheal, J. Billowes, M. L. Bissell, K. Blaum, F. C. Charlwood *et al.*, Phys. Rev. C **84**, 024303 (2011).
[9] K. Kaneko, T. Mizusaki, Y. Sun, and S. Tazaki, Phys. Rev. C **92**, 044331 (2015).
[10] J. C. Hardy, L. C. Carraz, B. Jonson, and P. G. Hansen, Phys. Lett. B **71**, 307 (1977).
[11] K. S. Krane, *Introductory Nuclear Physics* (Wiley, New York, 1988).
[12] T. Otsuka, T. Suzuki, R. Fujimoto, H. Grawe, and Y. Akaishi, Phys. Rev. Lett. **95**, 232502 (2005).
[13] J. Dobaczewski, N. Michel, W. Nazarewicz, M. Płoszajczak, and J. Rotureau, Prog. Part. Nucl. Phys. **59**, 432 (2007).
[14] R. P. de Groote, J. Billowes, C. L. Binnersley, M. L. Bissell, T. E. Cocolios, T. Day Goodacre *et al.*, Phys. Rev. C **96**, 041302(R) (2017).
[15] ENDSF database at the National Nuclear Data Center, http://www.nndc.bnl.gov.
[16] J. A. Winger, J. C. Hill, F. K. Wohn, E. K. Warburton, R. L. Gill, A. Piotrowski, R. B. Schuhmann, and D. S. Brenner, Phys. Rev. C **42**, 954 (1990).
[17] E. Browne and J. K. Tuli, Nucl. Data Sheets **111**, 1093 (2010).
[18] E. A. McCutchan, Nucl. Data Sheets **113**, 1735 (2012).
[19] G. Gürdal and E. A. McCutchan, Nucl. Data Sheets **136**, 1 (2016).
[20] D. Abriola and A. A. Sonzogni, Nucl. Data Sheets **111**, 1 (2010).
[21] B. Singh and A. R. Farhan, Nucl. Data Sheets **107**, 1923 (2006).
[22] B. Singh, Nucl. Data Sheets **74**, 63 (1995).
[23] A. R. Farhan and B. Singh, Nucl. Data Sheets **110**, 1917 (2009).
[24] B. Singh, Nucl. Data Sheets **105**, 223 (2005).
[25] J. L. Tracy, J. A. Winger, B. C. Rasco, U. Silwal, D. P. Siwakoti, K. P. Rykaczewski *et al.*, Phys. Rev. C **98**, 034309 (2018).
[26] Y. Shiga, K. Yoneda, D. Steppenbeck, N. Aoi, P. Doornenbal, J. Lee *et al.*, Phys. Rev. C **93**, 024320 (2016).
[27] M. Wang, G. Audi, F. G. Kondev, W. J. Huang, S. Naimi, and X. Xu, Chin. Phys. C **41**, 030003 (2017).
[28] U. Silwal, Ph.D. dissertation, Mississippi State University, 2018, ProQuest ETD 10980406.
[29] U. Silwal, S. V. Ilyushkin, J. A. Winger, K. P. Rykacezewski, C. J. Gross, J. C. Batchelder *et al.*, 2017 Fall Meeting of the APS Division of Nuclear Physics, Published Abstract KB.00004, http://meetings.aps.org/link/BAPS.2017.DNP.KB.4.
[30] R. Grzywacz, Nucl. Instrum. Methods Phys. Res., Sect. B **204**, 649 (2003).
[31] R. Grzywacz, C. J. Gross, A. Korgul, S. N. Liddick, C. Mazzocchi, R. D. Page, and K. Rykaczewski, Nucl. Instrum. Methods Phys. Res., Sect. B **261**, 1103 (2007).
[32] M. Lipoglavšek, A. Likar, M. Vencelj, T. Vidmar, R. A. Bark, E. Gueorguieve *et al.*, Nucl. Instrum. Methods Phys. Res., Sect. A **557**, 523 (2006).
[33] M. A. Schumaker, G. Hackman, C. J. Pearson, C. E. Svensson, C. Andreoiu, A. Andreyev *et al.*, Nucl. Instrum. Methods Phys. Res., Sect. A **570**, 437 (2007).
[34] U. Rizwan, A. B. Garnsworthy, C. Andreoiu, G. C. Ball, A. Chester, T. Domingo *et al.*, Nucl. Instrum. Methods Phys. Res., Sect. A **820**, 126 (2016).
[35] P. Hosmer, H. Schatz, A. Aprahamian, O. Arndt, R. R. C. Clement, A. Estrade *et al.*, Phys. Rev. C **82**, 025806 (2010).
[36] G. Rudstam, K. Aleklett, and L. Sihver, At. Data Nucl. Data Tables **53**, 1 (1993).

[37] D. C. Camp and B. P. Foster, Nucl. Phys. A **177**, 401 (1971).
[38] W. B. Walters (private communication).
[39] LOGFT program at National Nuclear Data Center, http://www.nndc.bnl.gov/logft/.
[40] B. A. Brown and W. D. M. Rae, Nucl. Data Sheets **120**, 115 (2014).
[41] M. Honma, T. Otsuka, T. Mizusaki, and M. Hjorth-Jensen, Phys. Rev. C **80**, 064323 (2009).
[42] V. K. Tikku and S. K. Mukherjee, J. Phys. G: Nucl. Phys. **1**, 446 (1975).
[43] J. Van Roosbroeck, H. DeWitte, M. Gorska, M. Huyse, K. Kruglov, K. Vande Vel *et al.*, Phys. Rev. C **69**, 034313 (2004).
[44] J.-C. Thomas, H. De Witte, M. Gorska, M. Huyse, K. Kruglov, Y. Kudryavtsev *et al.*, Phys. Rev. C **74**, 054309 (2006).
[45] A. M. Forney, W. B. Walters, C. J. Chiara, R. V.F. Janssens, A. D. Ayangeakaa, J. Sethi, J. Harker, M. Alcorta, M. P. Carpenter, G. Gurdal, C. R. Hoffman, B. P. Kay, F. G. Kondev, T. Lauritsen, C. J. Lister, E. A. McCutchan, A. M. Rogers, D. Seweryniak, I. Stefanescu, and S. Zhu, Phys. Rev. Lett. **120**, 212501 (2018).
[46] A. Chester, B. A. Brown, S. P. Burcher, M. P. Carpenter, J. J. Carroll, C. J. Chiara *et al.*, Phys. Rev. C **104**, 054314 (2021).
[47] S. Giraud, L. Canete, B. Bastin, A. Kankainen, A. F. Fantina, F. Gulminelli *et al.*, Phys. Lett. B **833**, 137309 (2022).